

# X-Ray Image Review of the Bone Remodeling Around an Osseointegrated Trans-femoral Implant and a Finite Element Simulation Case Study

WEI XU<sup>1</sup> and KINGSLEY ROBINSON<sup>2</sup>

<sup>1</sup>Centre for Biomedical Engineering, Faculty of Engineering and Physical Sciences, University of Surrey, Guildford, Surrey GU2 7XH, UK; and <sup>2</sup>Douglas Bader Unit, Queen Mary's Hospital, Roehampton, London SW15 5PN, UK

(Received 20 November 2006; accepted 21 December 2007; published online 16 January 2008)

**Abstract**—The insertion of an implant into a bone leads to stress/strain redistribution, hence bone remodeling occurs adjacent to the implant. The study of the bone remodeling around the osseointegration implants can predict the long-term clinical success of the implant. The clinical medial–lateral X-rays of 11 patients were reviewed. To eliminate geometrical distortion of different X-rays, they were converted into a digital format and geometrical correction was carried out. Furthermore, the finite element (FE) method was used to investigate how the bone remodeling was affected by the stress/strain distribution in the femur. The review of clinical X-rays showed cortical bone growth around the proximal end of the implant and absorption at the distal end of the femur. The FE simulation revealed the stress/strain distribution in the femur of a selected patient. This provided a biomechanical interpretation of the bone remodeling. The existing bone remodeling theories such as minimal strain and strain rate theories were unable to offer satisfactory explanation for the cortical bone growth at the implant side of the proximal femur, where the stress/strain level was much lower than the one in the intact side of the femur. The study established the correlation between stress/strain distribution obtained from FE simulations and the bone remodeling of the clinical review. The cortical bone growth was initiated by the stress/strain gradient in the bone. Through the review of clinical X-rays and FE simulations, the study confirmed that the bone remodeling in a femur with an implant was influenced by the stress/strain redistribution. The strain level and stress gradient hypothesis is presented to offer an explanation for the implanted cortical bone remodeling observed in this study.

**Keywords**—Bone remodeling, Osseointegration implant, Strain gradient, Finite element method.

## INTRODUCTION

Trans-femoral osseointegration implant is a new technique for prosthetic limb attachment with a percutaneous abutment. The advantages of using the

osseointegration technique, for the trans-femoral amputee's prosthetic limb attachment, include a full range of movement around the hip joint (which would normally be restricted by the conventional socket brim), reduced soft tissue problems and improved sensory feedback from the environment. Since 1997, in collaboration with the team in Sweden, a selected group of UK patients, for whom rehabilitation with conventional methods of prosthetic attachment has proved unsuccessful, have been undergone a clinical trial.<sup>19</sup> Eight years after the first UK patient had the osseointegration implant operation, the clinical X-rays of 11 UK amputees receiving osseointegration implant were reviewed, to investigate the bone remodeling developed around the implant region, which is the key to the long-term success of this new technique.

Bone is known, to be a dynamic tissue, which adapts to stress–strain changes by remodeling. This alters the overall shape of the mature bone as well as the internal architecture. The bone remodeling is an ongoing process, which is due to the interplay between osteoclastic and osteoblastic processes. The new bone matrix is formed by osteoblast deposition and the bone remodeling. This can be defined as a complex time-related biological adaptive process. Experimental evidence indicates that the bone remodeling is initiated by some biomechanical stimulus. For example, long-time bed rest,<sup>15</sup> disuse,<sup>9</sup> and weightlessness<sup>5</sup> will reduce the bone mass and growth rate. Similarly, intensive loading of the bone will increase the bone mass and geometry.

Previous bone remodeling studies led to two major theories about the biomechanical-induced bone remodeling process. The theory of the damage adaptive growth described the bone material as a classical mixture of solid material and fluid.<sup>2</sup> This was derived from the basic laws of continuum mechanics<sup>14</sup> and used the fatigue micro damage theory in an attempt to interpret the bone remodeling process. This used a stress induced micro damage and biological repairing model.<sup>7,16</sup> For the theory of stress/stain adaptive

Address correspondence to Wei Xu, Centre for Biomedical Engineering, Faculty of Engineering and Physical Sciences, University of Surrey, Guildford, Surrey GU2 7XH, UK. Electronic mail: w.xu@surrey.ac.uk

growth, various biomechanical components have been investigated as the remodeling stimulus, e.g., the stress,<sup>4,8</sup> strain energy density,<sup>11,22</sup> equivalent strain,<sup>18</sup> strain rate<sup>6</sup> and local stress nonuniformity,<sup>20</sup> and strain gradient.<sup>21</sup> These theories mainly consider the difference between actual value and reference value of the biomechanical stimulus as the driver of the bone remodeling process.

In addition to the biomechanical-based theories, the bone remodeling was also interpreted from the aspect of biological process. It should note that the biological process of the bone remodeling involves both mechanical and cellular factors. Fluid flow based stress/stain adaptive growth theory<sup>13</sup> provides a bridge to connect the mechanical stimulus effects and biological activities of the bone cell. The stress gradient introduced by the external load derives canalicular fluid flow in the bone and stimulates osteoclasts. The activities of osteoblasts result in bone remodeling.<sup>3</sup>

Despite various theoretical attempts to interpret the biomechanical-induced bone remodeling of the hip replacement, a systematic and quantitative investigation of the clinical bone remodeling process in an osseointegration implanted bone has not been previously reported. This study reviewed clinical X-rays of the first 11 UK patients who had received osseointegration trans-femoral implant operations in a period of 8 years. A digitized approach was developed to unveil the external bone remodeling process in terms of geometric changes. Due to individual variance and available X-rays, only the bone remodeling result of patient 4 was used for Finite element (FE) analysis of the relationship between implanted bone remodeling and stress redistribution. To understand the effect of biomechanical stimulus and predict the long-term bone remodeling process hence the success of the osseointegration implant, FE analysis was carried out to simulate the stress/strain distribution in the region of the osseointegration implant. With reference to the result of FE simulation, the existing bone remodeling theories were used to interpret results of the clinical review. It was found that at proximal region of the implant, the existing theories failed to explain the cortical bone growth observed from the clinical X-ray review. Consequently, the authors proposed a new hypothesis for implanted cortical bone remodeling in future studies.

## METHODS

### *Clinical X-Rays*

The clinical X-rays of this study were taken in accordance with the protocol for osseointegration assessment, once each year where possible and for

various clinical reasons such as infection, post-operative trauma and mechanical complications with the implant system. The X-rays were taken in two planes. In the anterior posterior (AP) view, the patient's stump was positioned so that image of the femur in the AP plane was obtained. In the medial-lateral (ML) position, the stump was turned 90° to expose the lateral surface of the limb and placed over the contralateral limb. However, comparing with AP position, the X-rays in the ML position were less consistent from session to session and patient to patient, while the X-rays were acquired, consideration was mainly given to the patient's ability to position/rotate the residual limb. This would introduce an angular distortion to the quantitative measurement of the cortical bone change from the X-rays in the ML position. Therefore, in this study, only X-rays in AP position were used. In addition to the angular distortion, the geometrical leveling and linear distortion between different sessions would also introduce inaccuracy, but this was corrected through the geometrical correction process described in the next section.

### *Geometrical Correction Procedure of the X-Ray Image*

Geometrical leveling and linear distortion between different sessions was inevitable, as the conventional X-ray was designed to provide a visible image rather than accurate dimensions of the object. Different clinical practices and settings could introduce various geometrical distortions. In order to eliminate the geometrical distortion between different clinical sessions, the X-rays were converted into digital format for a geometrical correction process. The geometrical correction of the X-ray images was carried out with reference to the diameter of the implant. This is because, in principle, the implant diameter of the same patient should not change from session to session. It provided a comparable geometrical reference to perform the correction. The geometrical correction of the X-ray images was carried out using PC software Photo Shop as it can also be used for quantitative measurement of X-ray images.

In the most clinical situations, the implant could not be guaranteed to be parallel with the film when the X-ray was taken. The X-ray image of the implant would appear to be distorted and the image length could be different as the real implant. To correct the X-ray image distortion, geometrical corrections were performed in two steps. The first step was leveling adjustment, which was to adjust X-ray image of the implant so that the implant image appeared to have a unique diameter. After the leveling adjustment, the implant image should have unique diameter along the length of the implant. The second step of the correction was to adjust the image length in the

**TABLE 1. Patients' information.**

Patient	Amputation side	Age at time of implantation	Height (cm)	Weight (kg)	Insertion time	Amputation time prior to implantation (year)
1	Left	15/5/66	170	100	16/1/97	13
2	Right	9/2/71	170	49	06/97	5
3	Left	12/3/68	170	84	18/9/97	4
4	Right	18/4/73	170	76	4/2/98	3
5	Right	4/9/72	180	85	3/2/98	8
6	Left	16/7/67	180	79	18/4/00	10
7	Left	10/2/60	162	60	19/4/00	5
8	Right	4/8/70	170	76	19/4/00	10
9	Right	19/2/63	168	75	24/4/02	15
10	Right	11/9/59	173	95	25/4/02	12
11	Right	33	178	93	25/4/02	7

longitude direction to match the length of the real implant provided by the manufacturer. The conventional orthopedic X-ray image would normally be slightly enlarged due to the limited distance between the point X-ray source and bone, and the distance between the implanted bone and X-ray film. As the result, the diameter of the implant image needs to be corrected as well. The third step of geometrical correction was to scale the image in the diameter, to match the diameter of the implant image with real implant.

*Bone Remodeling Review*

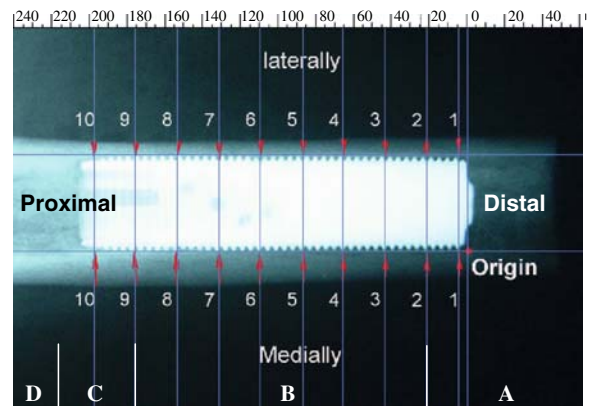
This study was divided into a general review and a detail study, which is a designated measurement of the cortical bone thickness changes after the implant was inserted. The X-rays for the general review were from the clinical files of 11 UK osseointegration patients. It was to confirm the trend of the bone remodeling at the distal and proximal end of the implanted femurs. The designated cortical bone measurement was performed on the X-rays of a selected patient. It provided quantitative cortical bone thickness change in the osseointegration patients. Table 1 lists detailed information of all the 11 patients in this study.

Table 2 lists the patient number, time of the X-rays and the time of the implantation. For the general review, the bone thickness changes were measured between the first available X-ray and subsequent X-rays. As the time interval varied significantly from patient to patient, the assessment only provided a qualitative trend for the bone modeling.

For the detail study, bone remodeling around the implant region was measured by cortical bone thickness change in a selected patient. Patient 4 in Table 2 was selected for this designated review, as this patient had relatively regular and evenly spaced X-rays over a period of 7 years. The bone remodeling

**TABLE 2. Clinical X-ray times of 11 UK patients.**

Patient number	X-ray time after the first operation (Year + Month)
1	7M; 1Y9M; 1Y11; 3Y6M; 3Y9M
2	11M; 1Y6M; 2Y4M
3	2Y; 2Y3M; 3Y1M; 5Y1M; 5Y5M
4	1M; 6M; 10M; 2Y8M; 3Y8M; 4Y5M; 5Y6M; 6Y10M
5	5M; 1Y1M; 1Y4M; 1Y6M
6	6M; 1Y6M; 2Y5M; 3Y1M
7	1Y10M; 2Y4M; 2Y6M; 3Y
8	6M; 1Y6M; 2Y 4M; 2Y9M
9	6M; 1Y
10	6M;10M
11	6M; 10M



**FIGURE 1. A geometrically corrected clinical X-ray image.**

development was measured with respect to the duration of the osseointegration implant. The cortical bone thickness measurements were carried out on the geometrically corrected X-ray images. As shown in Fig. 1, the cortical bone thickness changes were measured at 10 different locations along the diaphysis of the femur. A manual measurement was used,

because a computerized program had difficulties handling the nonuniform grey scale from different X-rays. The actual measurements were performed on digital images enlarged four times to improve visibility. In order to maintain high accuracy and reliability, at each location, the measurement was repeated three times. The average of the three measurements was used. The bone thickness measurement was only performed in medial and lateral two positions of the AP X-rays as the ML X-rays would introduce an inconvertible angular distortion.

*Finite Element analysis*

As mentioned in the “Introduction” section, a biomechanical environment change, in particular stress and strain, can initiate a bone remodeling. The purpose of FE analysis was to simulate the stress/strain distribution around the implant and to identify the key factors that initiated the bone remodeling phenomena observed in this study. The FE analysis was performed on a femoral-implant model from the same patient selected for the cortical bone thickness measurement study. According to the current procedure in the UK osseointegration clinical trial, there was no CT scan after the threaded implant was inserted. The 3D femoral model used for the FE analysis was reconstructed from the patient’s pre-operation CT scans and the position of the implant in the femur was based on the first X-rays after the implant was inserted.

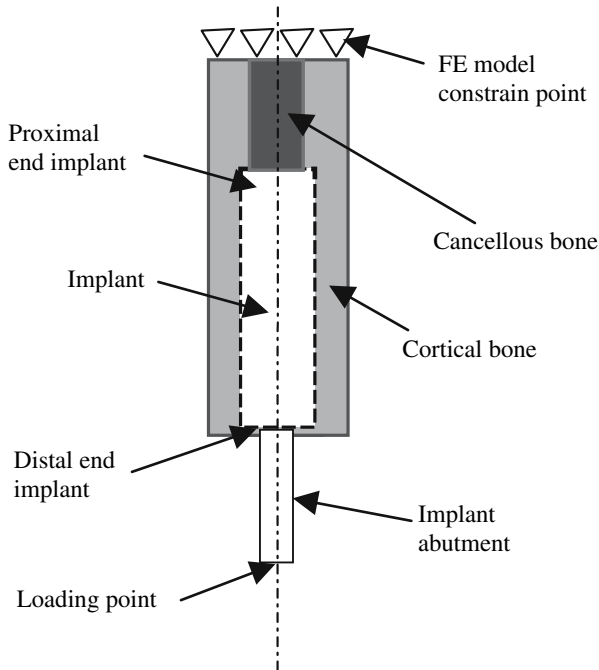


FIGURE 2. Boundary conditions of the femur-implant model.

The material properties of the FE femoral model were the same as those in the author’s previous publication.<sup>23</sup> The diaphysis of the cortical bone was modeled to be transversely isotropic with a constant longitudinal elastic modulus of 18 GPa, circumferential elastic modulus of 13 GPa, and a shear modulus of 7 GPa. The Poisson’s ratio of the cortical bone was 0.3. The elastic modulus of cancellous bone varying with its density, 0.35 GPa was used in the diaphysis area. The implant was commercially pure (CP) titanium with elastic modulus of 110 GPa and Poisson’s ratio 0.3. A load combination of axial compression force (3750 N), torsion (20 N m), flexion/extension (60 N m), and abduction (40 N m). Bending moments were applied to the femur-implant model. This load combination represented typical forces and moments experienced on the knee at 20% of the gait cycle during normal walking of a person weighing 75 kg,<sup>1,12</sup> which was close to the patient’s body weight of 76 kg. The loading and constrain points on the FE model are shown in the Fig. 2. To simulate well-established osseointegration between femur and implant, the elements represent the bone and implant models were modeled to share the same nodes.<sup>23</sup>

**RESULTS**

*Review of Bone Thickness Change*

The general review of bone remodeling was focused on the distal and proximal end of the implant as the inserted implant led to significant stress redistribution in these areas. This was carried out by the measurement of cortical bone thickness change between each patient’s first and subsequent X-rays listed Table 2. Figure 3 plots the maximal change of the cortical bone growth and absorption in distal medial (DM), distal

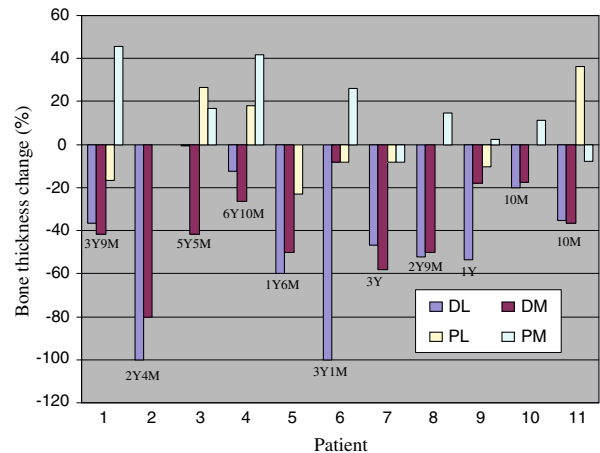


FIGURE 3. Maximal cortical bone changes at distal and proximal implant areas.



lateral (DL), proximal medial (PM), and proximal lateral (PL) sides. The maximal reading error between each measurement was 0.1 mm. With respect to the duration of the implant, there was a general trend of bone absorption at the distal end and bone growth around the proximal end. However, the trend of bone absorption at the distal end was more obvious than the bone growth at the proximal end.

It should be noted that Fig. 3 only demonstrated a general trend for bone remodeling around the distal and proximal end of the implant. An inter-patient comparison was impossible, as the time span between the first and subsequent X-rays of each individual patient was inconsistent.

#### *Bone Remodeling in the Selected Patient*

Figure 4 shows eight X-rays of the selected patient from this study. The X-rays were taken during a period of 7 years after the trans-femoral osseointegration implant was inserted. The dates of the X-rays are shown on the figure. The first X-ray was 51 days after the implant was inserted. The intervals between this first post-operation X-ray and the subsequent ones were 9, 19, 31, 40, 53, 56, and 69 months. All the X-rays were geometrically corrected according to the

procedure described in “Methods” section and bone thickness change measurements were then carried out on these X-ray digital images.

Compared with the general review of all 11 UK patients, the measurement of cortical bone thickness change in the selected patient were correlated to the duration of the implant, which provided clinical evidence of quantitative bone remodeling process after the osseointegration implant was inserted. The measured bone thickness from the X-ray images in medial and lateral sides of femur are shown in Figs. 5a and 5b, respectively. In the figures, there were eight curves representing different times when X-rays (used for bone thickness measurement) were taken. The horizontal axis defines (from right to left) the distance from distal to proximal end of the implant/femur. The vertical axis corresponds to the cortical bone thickness measured at the different times when X-rays were taken.

The result showed that, at position 1, the cortical bone thickness was reduced over the time while at the position 10 the bone thickness increased over the time. Around the middle femoral diaphysis, no significant change was found at the early stage, but the longer the implant was in place, the cortical bone thickness in this region began to increase while the cortical bone at the

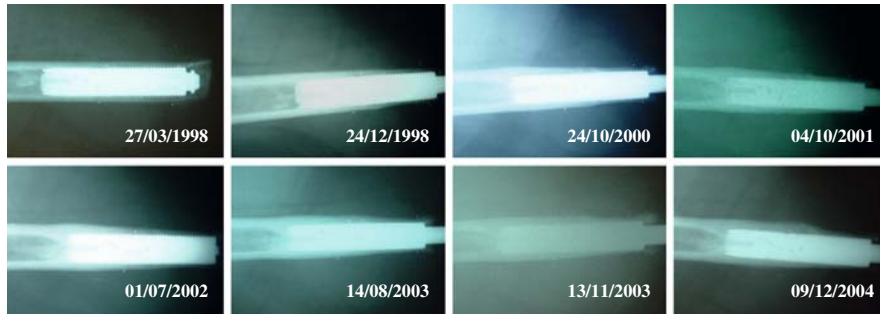


FIGURE 4. Clinical X-rays of the selected patient for a period of 7 years.

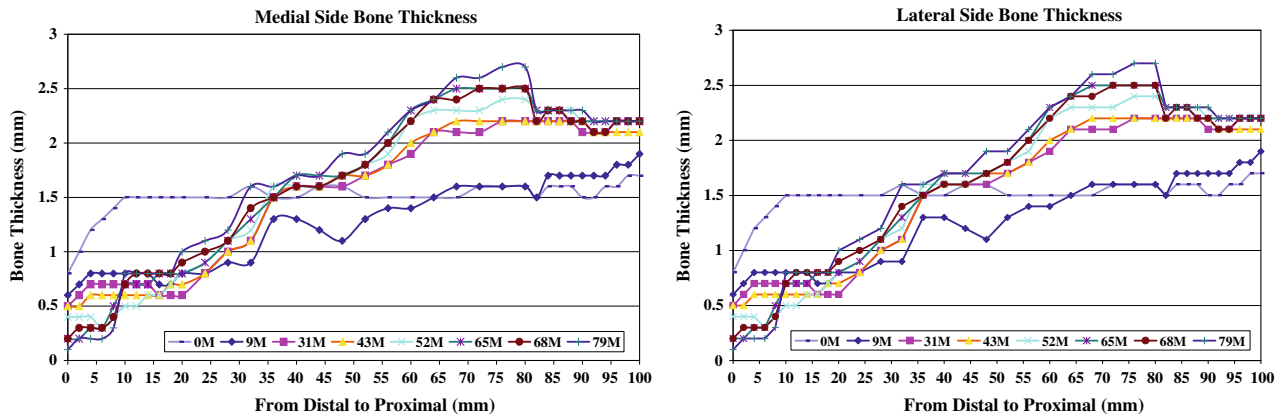


FIGURE 5. Cortical bone thickness change in medial and lateral sides of the femur of the selected patient.

distal end continued the trend of absorption. Compared with the lateral side, the bone around proximal end of implant showed a higher growth rate in the medial side.

*FE Simulation of the Selected Patient*

The FE analyses were carried out using a femur-implant model of the selected patient. The model was held at the proximal end and a typical walking load combination, described in “Finite Element Analysis” section, was applied to the abutment of the implant as shown in Fig. 2. The FE simulations were carried out using both intact and implanted femur for biomechanical comparison. Von Mises stress and equivalent strain were used to present the stress/strain level and distribution in the femur. For an anisotropic femur, Von Mises stress is not the most relevant measure of mechanical stimulus, but it has been used to charac-

terize the bone loading as it provides a convenient scalar representation of the stress state<sup>23</sup> and used by the most of previous publications. As comparison, Fig. 7 shows both Von Mises equivalent strain and the principal stress.

Figure 6 plots the Von Mises stress distribution contour in A–P plane of the femur. A stress concentration can be found near to the proximal femur where the implant ends.

It should be noted that under the typical walking load, the maximal stress plane is at 33.7° clockwise from the A–P plane. As the X-rays were filmed in A–P plane, this study focused on the stress/stain level and distribution in the A–P plane. This would allow a correlation study to be carried out between the stress/stain level, distribution and the bone remodeling in the A–P plane.

Figure 7 shows the Von Mises equivalent strain level on the medial surface along the femur diaphysis of an implanted and intact femur-implant models. Around the proximal end of the femur (region C), the strain level reaches a peak value at the place where the implant ended. Moving toward to the femoral head direction (region D), the strain returns to the level same as in the intact femur. However, toward the distal direction (region B), the strain drops to a lower level and remains the same along the femoral diaphysis before it drops further to zero where it approaches the distal end of the femur (region A).

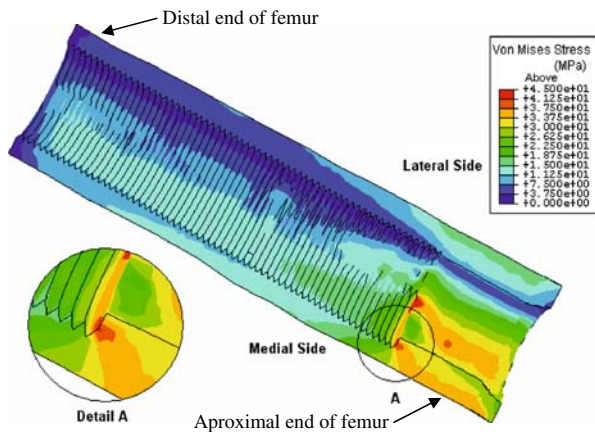
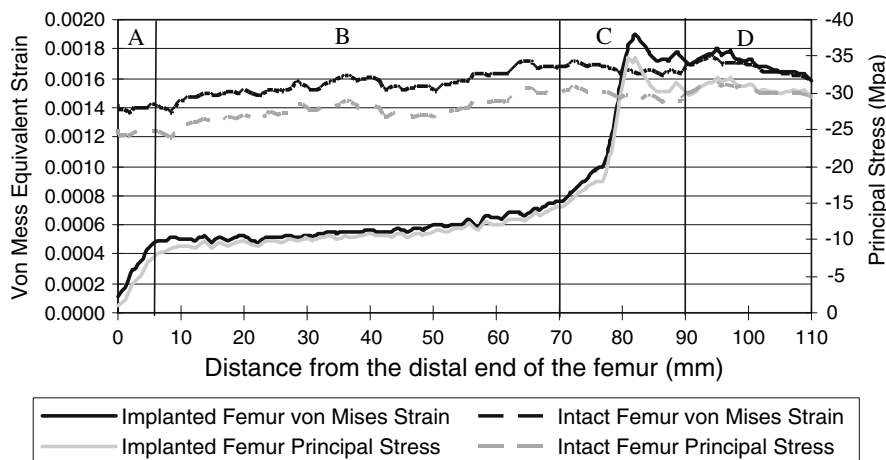


**FIGURE 6.** Stress distribution along the femur diaphysis.

**DISCUSSION**

*The Bone Remodeling*

From Table 2, it can be seen that patients 1, 2, 3, 5, and 6 had the first X-rays 7, 11, 24, 5, and 6 months,



A-distal region, B-diaphysis region, C- region close to the end of implant and D-intact region

**FIGURE 7.** Von Miss Equivalent strain and principal stress levels on the medial surface of the femoral diaphysis.

respectively, after the implants were inserted, while the others had the first X-rays after less than 1 month. An inter-patient comparison shown in Fig. 3 should only be used for presenting a general trend of the bone remodeling since the time of the first X-ray and time intervals between X-rays varied significantly from patient to patient. And a quantitative study should be based on the patient with more informative X-rays. Nevertheless, the review of the X-rays of the 11 UK patients over a period of 8 years indicates following trends of the bone remodeling process around the osseointegration implant.

At the distal end, cortical bone absorption was observed in the most of the X-rays. The highest absorption was 100% of original bone thickness of the patient 2 and 6. The average absorption rates of patients 2 and 6 were 3.57% and 2.7% per month. However, patient 9 had the highest absorption rate, which was 53.4% in 12 months, i.e., 4.45% per month. At the proximal end, cortical bone growth was observed from X-rays of some patients. Three showed fast cortical bone growth at the proximal end of implant were 45.8%, 41.7%, and 36.2% of patients 1, 4, and 9 in 45, 69, and 10 months, respectively. Patient 9 had the fastest growth rate, which was 3.6% per month. Meanwhile, no clear correlation was identified between the bone remodeling and patient's age, weight, height, and implant service time listed in Table 1.

At the proximal end of the implant, the cortical bone growth was not observed on X-rays of patients 2 and 6. This was because the implant of patients 2 and 6 were removed due to failure of the osseointegration caused by unhealed previous cortical bone fracture. The explanation for this was that failure of the bone-implant osseointegration had restricted the use of the prosthetic limb, which had prevented the residual femur from experiencing the necessary load and a healthy bone remodeling process.

It should be noted that a small amount of bone absorption was found at the proximal end of implant on the X-rays of patient 1, 6, 7, 9, and 11. A possible cause of this was the angular inconsistency between each X-ray in the A-P plane. Although geometrical correction was performed with minimal linear inaccuracy, it was not possible to correct this angular inconsistency. This limitation needs to be overcome in the future study.

#### *Influence of the Biomechanical Environment*

Following the general review of the clinical X-rays of the 11 UK trans-femoral osseointegration patients, patient number 4 listed in Table 2 was selected for quantitative study of the cortical bone thickness change along the implanted femoral diaphysis. The FE

analysis was performed to simulate the stress redistribution in the femoral region after an osseointegration implant is inserted. Correlation was sought between the biomechanical environment change and the cortical bone remodeling process.

Figure 5 shows the cortical bone thickness change against the duration of the implant. The bone absorption at the distal end of femur and bone growth around the proximal end of implant were consistent with trend of bone remodeling obtained from the general review of 11 UK patients. It was suggested that the bone absorption at the distal end was caused by stress shielding, as the inserted implant carried the most of load on the limb. Compared with the load upon a health limb the implanted femur was less stressed. It is known that a minimal strain level is required to maintain a balanced bone remodeling. According to previous studies, a healthy strain level for human bone is between of 1,000 and 500 micro strain.<sup>10,17</sup>

As shown in Fig. 7, the Von Mises equivalent strain level on the medial surface of the residue femur confirms that, at the distal end of the femur, the strain has dropped below the level to maintain a balanced bone remodeling process. Along the femoral diaphysis, the strain level is slightly higher than the 500 micro strain, therefore no bone absorption was observed.

Unlike the distal end, Fig. 5 shows that the cortical bone thickness at the proximal end increases as the implant service time increases. It is worthwhile to point out that apart from a small strain peak at the proximal end of implant (corresponding to the region C in Fig. 7), the strain level in this area is lower than the same region on the intact femur and the region beyond the implant (region D in Fig. 7). However, the cortical bone thickness in this region increased, while the cortical bone thickness kept the same in the region beyond the implant (region D in Fig 7). The region C can be divided into two sub-regions, which are from 70 to 80 mm and 80 to 90 mm. The FE simulation shows that the strain level in the first region is increased from 800 to 1700 micro strain and the strain reaches a peak value in the second sub-region. Compared with the strain level in the intact femur and the region D, the strain level in the first sub-region is lower. Even in the second sub-region of the region C, the average strain level is only around 1800 micro strain. This raises an argument against the existing bone remodeling theory, which assumes the difference between actual and reference biomedical stimulus was considered to be the driver of the bone remodeling (growth or absorption).

To identify the exact driver of the bone growth in the region C, the correlation between the FE result (Fig. 7) and the bone thickness change (Fig. 5) was examined. It was found that the bone growth in the region C, especially its first sub-region, was closely

related to the stress gradient in the region. This correlation could be generally explained by the fluid flow based stress/stain adaptive growth theory.<sup>13</sup> It assumes that the stress gradient is the driver of the bone growth.<sup>3</sup> However, at the region A, where the FE result (Fig. 7) plots a high stress gradient, the bone absorption took place. Clearly the fluid flow based stress gradient theory is unable to provide an adequate interpretation to the clinical review and FE results in the region A.

Figure 6 shows that in the areas corresponding to a large cortical bone thickness increase in Fig. 5, a stress concentration is observed. Figure 6 shows that stress has a significant change from 4.1 to 1.8 MPa around the proximal end of the implant. The authors believe that the bone remodeling observed from the clinical review of X-rays and stress redistribution from the FE simulation supports such a hypothesis that the bone remodeling is initiated by the stress gradient perpendicular to direction of bone remodeling. However, the stress gradient seemed to be only contributing to the bone growth when the stress level above a certain value. When the stress was below a certain value, strain level became dominant factor of the bone remodeling. The bone absorption in the region A was the result of this.

#### *The Variability of Bone Remodeling Review and the Limitation of the Study*

Although the FE simulation correlates with the general trend of the review of the X-ray images, there are significant differences of bone remodeling among patients who have the same insertion time. The study showed that the evidence of bone absorption around the distal end was more obvious than the bone growth around the proximal end. The bone absorption took place around some patient's proximal region, for example, patients 7 and 11 showed absorption in the PM region, and patients 1, 5, 6, 7, and 9 showed absorption in the PL region, whereas it was more understandable that patients 3, 4, and 11 showed bone growth in the PL region where high stress gradient existed. The explanation for this is that the individual biological variability, such as age, hormone, bone growth factors and calcium-phosphorus metabolism, and nature of prosthetic limb usage. The former one is beyond the theme of this study. While the later one contributes to the dynamic loading pattern put upon the osseointegration implant system. It is suggested that the dynamic loading, which creates a certain level of strain rate is a critical factor to ensure health bone remodeling.<sup>6</sup> Restricted by the limited physiological information and walking style (i.e., usage of prosthetic limb) of individual patients, it is hard to make an exclusive interpretation of the above-mentioned cases.

It should be noted that, in this study, the strain/stress adaptive bone remodeling theory was cited by the authors' to discuss the findings. This was because the damage adaptive growth theory used accumulating damage stimulus as the remodeling driver, which was the result of the mechanical factor. Therefore, the damage adaptive theory was more suitable to predict bone density remodeling.

Finally, one of the other major limitations of this study, is that only one patient was selected for the case study of the FE simulation. More cases would need to develop a formula for the bone remodeling mechanism, which could provide a measurable support for the hypothesis of this study.

## CONCLUSIONS

The clinical X-ray review in this study shows the bone remodeling process in the residual femur of osseointegration patients over a period of 8 years. The FE simulation result confirmed that the bone remodeling in an implanted femur was influenced by the stress/strain redistribution. The stress/strain adaptive bone remodeling theory could be used to explain the bone absorption caused by stress shielding at the distal of the femur. The fluid flow base stress gradient theories could be used to interpret the bone growth at the proximal end. However, there is no unique bone remodeling theory, which offers satisfactory explanation for the bone absorption at the distal end and bone growth around the proximal end. The author's new hypothesis suggested that the bone remodeling was initiated by two factors: overall stress/strain level and stress gradient. When the stress/strain is below a certain level, it regulates the bone absorption. When the stress is above a certain level the stress gradient regulates the bone growth. This hypothesis reflects a new understanding of the cause of external remodeling of a femur containing an implant.

## REFERENCES

- <sup>1</sup>Baumann, J. U., A. Schar, and G. Meier. Reaction forces and moments at hip and knee. *Orthopade* 21(1):29-34, 1992.
- <sup>2</sup>Baumgartner, A., and C. Mattheck, Computer simulation of the remodelling of trabecular bone. In: *Computers in Biomedicine*, edited by K. D. Held, C. A. Brebbia, and R. D. Ciskowski. Southampton: Computational Mechanics Publications, 1991, pp. 291-296.
- <sup>3</sup>Burger, E. H., J. Klein-Nulend, and T. H. Smit. Strain-derived canalicular fluid flow regulates osteoclast activity in a remodeling osteon—a proposal. *J. Biomech.* 36(10): 1453-1459, 2003.



- <sup>4</sup>Carter, D. R., M. C. H. Van der Meulen, and G. S. Beaupre. Mechanical factors in bone growth and development. *Bone* 18(1):S5–S10, 1996.
- <sup>5</sup>Collet, P., D. Uebelhart, L. Vico, L. Moro, D. Hartmann, M. Roth, and C. Alexandre. Effects of 1-and 6-month spaceflight on bone mass and biochemistry in two human. *Bone* 20(6):547–551, 1997.
- <sup>6</sup>Cowin, S. C. *Bone Mechanics*. Boca Raton, Florida: CRC Press, 1990.
- <sup>7</sup>Doblaré, M., and J. García. Application of an anisotropic bone-remodeling model based on a damage-repair theory to the analysis of the proximal femur before and after total hip replacement. *J. Biomech.* 34(9):1157–1170, 2001.
- <sup>8</sup>Fischer, K. J., C. R. Jacobs, M. E. Levenston, and D. R. Carter. Observations of convergence and uniqueness of node-based bone remodeling simulations. *Annl. Biomed. Eng.* 25(2):261–268, 1997.
- <sup>9</sup>Hazelwood, S. J., R. B. Martin, M. M. Rashid, and J. J. Rodrigo. A mechanistic model for the internal bone remodeling exhibits different dynamic responses in disuse and overload. *J. Biomech.* 34:299–308, 2001.
- <sup>10</sup>Huiskes, R. Biomechanics of bone implant interactions. In: *Frontiers of Biomechanics*, edited by S. Schmid. Springer-Verlag, New York, 1986.
- <sup>11</sup>Kerner, J., R. Huiskes, G. H. van Lenthe, H. Weinans, B. van Rietbergen, C. A. Engh, and A. A Amis. Correlation between pre-operative periprosthetic bone density and post-operative bone loss in THA can be explained by strain-adaptive remodeling. *J. Biomech.* 32(7):695–703, 1999.
- <sup>12</sup>Kowalk, D. L., J. A. Duncan, and C. L. Vaughan. Abduction-adduction moments at the knee during stair ascent and descent. *J. Biomech.* 29(3):383–388, 1996.
- <sup>13</sup>Kufahl, R. H., and S. Saha. A theoretical-model for stress-generated fluid-flow in the canaliculi lagunae network in bone tissue. *J. Biomech.* 23(2):171–180, 1990.
- <sup>14</sup>Mattheck, C., and H. Huber-Betzer. CAO: computer simulation of adaptive growth in bones and trees. In: *Computers in Biomedicine*, edited by K. D. Held, C. A. Brebbia, and R. D. Ciskowski. Southampton: Computational Mechanics Publications, 1991, pp. 243–252.
- <sup>15</sup>Nishimura, Y., H. Fukuoka, M. Kiriyama, Y. Suzuki, K. Oyama, S. Ikawa, M. Higurashi, and A. Gunji. Bone turnover and calcium metabolism during 20 days bed rest in young healthy males and females. *Acta Physiol. Scand.* 150(S616):27–35, 1994.
- <sup>16</sup>Prendergast, P., and D. Taylor. Prediction of bone adaptation using damage accumulation. *J. Biomech.* 27(8):1067–1076, 1994.
- <sup>17</sup>Rubin, C. T., and L. E. Lanyon. Biological Modulation of Mechanical Influences in Bone Remodeling. In: *Biomechanics of Diarthroidal Joints*, edited by V. C. Mow. New York: Springer-Verlag, 1990.
- <sup>18</sup>Stülpmner, M. A., B. D. Reddy, G. R. Starke, and A. Spirakis. A three-dimensional finite analysis of adaptive remodeling in the proximal femur. *J. Biomech.* 30(10):1063–1066, 1997.
- <sup>19</sup>Sullivan, J., M. Uden, K. P. Robinson, and S. Sooria-kumaran. Rehabilitation of the trans-femoral amputee with an osseointegrated prosthesis: the United Kingdom experience. *Prosthet. Orthot. Int.* 27(2):114–120, 2003.
- <sup>20</sup>Tsubota, K., T. Adachi, and Y Tomita. Functional adaptation of cancellous bone in human proximal femur predicted by trabecular surface remodeling simulation toward uniform stress state. *J. Biomech.* 35(12):1541–1551, 2002.
- <sup>21</sup>Turner, C. H., V. Anne, and R. Pidaparti. A uniform strain criterion for trabecular bone adaptation: Do continuum-level strain gradients drive adaptation. *J. Biomech.* 30(6):555–563, 1997.
- <sup>22</sup>Weinans, H., R. Huiskes, and H. J. Grootenboer. The behaviour of adaptive bone-remodeling simulation models. *J. Biomech.* 25:1425–1441, 1992.
- <sup>23</sup>Xu, W., A. Crocombe, and S. Hughes. Finite element analysis of bone stress and strain around a distal osseointegrated implant for prosthetic limb attachment. *Proc. Inst. Mech. Eng. H J. Eng. Med.* 214:595–602, 2000.